npj | biosensing

Perspective

https://doi.org/10.1038/s44328-026-00112-y

Opioid sensing at point-of-need

Thinh Q. Bui[1] ✉, Edward R. Sisco[2], Kyle D. Chapkin[1,3], Wenqi Zhu[1], Junyeob Song[1], Dhruv Forma[4], Anthony J. Kearsley[5] & Henri J. Lezec[1]

The opioid epidemic—headlined by synthetic fentanyl—is a growing international crisis. NIST has been tasked with leading the analytical effort to better understand the evolving illicit drug landscape. We describe initiatives to advance portable mass spectrometry and develop metamaterial-enhanced spectroscopy, integrated with advanced modeling. Together, these programs support a comprehensive strategy that emphasizes measurement science and data standardization as essential tools for combating the growing threat of synthetic opioids.

Opioids for pain management and treatment are prevalent in medicinal therapeutics for a wide range of health conditions. Unfortunately, this reliance has also driven opioid dependence and abuse, resulting in an epidemic affecting major nations across the world[1]. In the United States alone, the surge in influx and abuse of opioids, especially illicitly manufactured fentanyl, nitazenes, and more recently orphines, pose a major health crisis, causing over 54,000 opioid deaths (≈ 80,000 drug overdose deaths in total) in 2024[2] and inflicting an economic impact of nearly 1.5 trillion USD[3].

As drug overdose deaths continue to remain near historic highs, understanding the dynamic illicit drug landscape has become a priority for both law enforcement and public health agencies. In December 2023, the Testing, Rapid Analysis, and Narcotic Quality (TRANQ) Research Act (https://www.congress.gov/bill/118th-congress/house-bill/1734.) was signed into law that mandates the National Institute of Standards and Technology (NIST) to (1) undertake research activities to develop emerging technologies for rapid, real-time drug detection of novel synthetic opioids and (2) engage with government (local, state, and federal) and law enforcement agencies to help advance their detection capabilities and establish standardized data workflows to keep up with the evolving illicit drug supply. Most importantly, this law calls for NIST to engage with public health entities, emergency responders, and law enforcement agencies at the forefront of the opioid crisis to amplify their research efforts and missions.

The analysis of illicit drugs is a monumental undertaking - involving agencies from border interdiction to law enforcement to public health and emergency medicine at the local, state, federal, academic, and non-profit levels. Each entity within this ecosystem is trying to address a particular need (e.g., prevent mass overdoses or interdict illicit substances at the border) in varying operational conditions. To provide some context to the size of this effort, in 2024, the approximately 400 state and local forensic science laboratories in the U.S. analyzed 1.1 million drug items submitted by law enforcement (https://www.nflis.deadiversion.usdoj.gov/home.xhtml.). This volume of samples, alone, is enough to drive up backlogs at laboratories. Add to it the fact that the drug landscape is constantly changing[4] - driven by the synthesis of novel, often more potent compounds - and one can see why detection and identification efforts have become difficult in both in the field and in the laboratory.

As the drug epidemic continues, cracks in the analytical backbone supporting detection and identification efforts grow. Today, the main analytical tools for identification and quantification of drug samples are mass spectrometry (typically laboratory based and coupled with chromatography) and spectroscopy (typically field-based and either Fourier-transform infrared spectroscopy (FTIR) or Raman spectroscopy). There is an urgent need for the next generation of advanced analytical methods better suited for rapid analysis of chemically-complex and ever-changing samples. Tools that have potential for mobile applications (rapid diagnostics at point-of-need) will be advantageous, but must meet many needs including low cost, low sensitivity, high specificity, and low operational complexity. In this work, we discuss current efforts at NIST to develop or accelerate and emerging technologies and standardized data workflows to advance portable drug sensing to meet the encompassing goals of the TRANQ Research Act.

Needs and challenges

The need for advanced instrumental and data analytics is driven by both the challenges in chemical composition of the sample itself and the desired end use of the data. In recent years, the complexity of the street drug market has increased, and this has been especially prominent with opioids. The TRANQ Research Act explicitly targets fentanyl and related opioids as a national security priority and calls for the development of validated and standardized approaches towards active detection, identification, and monitoring of these drugs in the United States. In the 2010's, a rapid rise in the number of fentanyl analogs (compounds with one or more structural modifications to the core fentanyl backbone), highlighted limitations in analytical techniques that are based on spectral libraries. During this time, laboratories and instrument manufacturers were unable to obtain chemical standards and update spectral libraries at the pace of new compounds

[1]Physical Measurement Laboratory, National Institute of Standards and Technology, Gaithersburg, MD, USA. [2]Material Measurement Laboratory, National Institute of Standards and Technology, Gaithersburg, MD, USA. [3]Department of Chemistry, University of Maryland, College Park, MD, USA. [4]Xanadu Quantum Technologies, Toronto, ON, Canada. [5]Information Technology Laboratory, National Institute of Standards and Technology, Gaithersburg, MD, USA.
✉e-mail: thinh.bui@nist.gov

emerging. This issue continues to this day, now driven by the influx of synthetic opioids belonging to the nitazene[5] and orphine[6] classes. Many of these compounds are more potent than fentanyl, leading to lower overall concentrations of synthetic opioids in street samples, often hindering detection capabilities. This also leads to a high proportion of other active and inactive ingredients in a street drug sample. These other compounds can encompass everything from inert ingredients like mannitol or microcrystalline cellulose to active ingredients like benzodiazepines or other sedatives designed to extend the high, numb the injection site, or reduce the negative side effects of withdrawal. Synthesis byproducts and unreacted precursors are also often present.

While analytically challenging, the complexity of the drug mixtures can provide a wealth of information[7]. The adulterants in the drug mixture, and their relative proportions, may provide information on samples coming from similar sources or information on what point in the supply chain a material was interdicted. The byproduct and precursor information can provide insights into how the opioids were manufactured. Other chemical information (e.g., isotope measurements) can potentially geolocate manufacturing. This type of information, which can map the movement of drugs within the drug supply, is critical not only for intelligence and interdiction efforts but also for overdose prediction and prevention.

Current real-time analysis of drugs, today, often relies on fentanyl immunoassay test strips[8], or color tests[9]. Test strips only provide information on the presence or absence of fentanyl, and may be prone to false positive or negative results. Color tests have similar limitations, as they provide information on the presence of specific chemical moieties[9]. FTIR or Raman spectroscopy is often used in conjunction for more expedited chemical screening, but these techniques typically only provide information about major components in the mixture and may lack the detection sensitivity for minor and potentially toxic synthetic opioids[4]. Due to its impressive detection sensitivity, mass spectrometry, typically coupled with gas or liquid chromatography, is the gold standard for confirmatory drug analysis, but the instrumentation is costly, complex, and bulky (limited mobility), and is typically housed in sophisticated laboratories. Perhaps most importantly, for all of these analytical techniques there are no standard methods or analysis protocols, which complicates the ability to combine data from multiple data streams or multiple entities using the same analytical tool.

The importance of real-time data drug data cannot be understated, as up-to-date data can inform immediate appropriate action (overdose prevention, interdiction, etc.), and long-term aggregated data can provide insights on broader questions (trend analysis, forecasting, and data mining). This urgent need continues to drive advances in analytical techniques to provide rapid access to accurate and quantitative chemical data. New tools for drug screening are always desirable, but one that can be readily adopted, validated, and implemented are other difficult barriers to entry. Despite these challenges, emerging tools that overcome a number of key limitations of existing technologies while providing fit-for-purpose capabilities can play a key role for the task at hand. In response to the TRANQ Research Act's call for near real-time drug monitoring, NIST is pursuing a dual-track strategy: (1) developing novel metamaterial-based spectroscopic technologies for rapid, field-deployable drug detection and (2) accelerating portable mass spectrometry platforms as pilot systems for next-generation mobile drug checking. Achieving comprehensive testing also requires quantitative concentration information for understanding potency and dosage, rather than just compound identification, and therefore is also being studied. Creation of a mobile laboratory, to provide comprehensive point-of-need analysis and aid in technology development, is also underway.

Analytical tools

Portable mass spectrometry

Mass spectrometry is currently the most prevalent tool for both presumptive and confirmatory identification of drugs. Measurement of opioids using mass spectrometry involves highly sensitive and selective analytical techniques that enable qualitative identification and/or quantitative determination of opioid compounds in complex biological or drug product samples. Driving needs for continued development in mass spectrometry are focused on improving speed, specificity, and real-time detection across diverse matrices (chemical or biological).

A growing body of research has demonstrated that ambient ionization mass spectrometry (AI-MS)[10] has the potential to address the speed and real-time detection needs. Figure 1 provides an overview of NIST's current mass spectrometry capabilities. This growing technology space, where samples are directly desorbed or dissolved under ambient conditions before transport to a mass spectrometer encompass many prototype and several commercially-available systems. One type of AI-MS system that has been of particular interest, due to its adoption by forensic laboratories, is direct analysis in real-time mass spectrometry (DART-MS[11,12]). DART-MS has become a workhorse for rapid, chromatography-free screening directly from bulk or trace samples. Adoption of this type of analysis was driven, in part, by efforts at NIST to lower the implementation barriers of new technologies, through the creation of validation templates[13], spectral libraries[14], and spectral search algorithms[15,16] to streamline implementation of AI-MS by relevant agencies.

Active research is also focused on integrating miniaturized, portable mass spectrometers for on-site opioid testing in clinical, forensic, and law enforcement settings. These systems can reduce analysis times from hours to minutes while providing front-line personnel with information-rich data. For example, a recent study demonstrated rapid in-field drug analysis using a field-deployable DART-MS platform[17]. The ruggedized time-of-flight mass spectrometer was shown to have similar performance metrics to laboratory-based systems. Given the complexity of samples, and the fact that isobaric interferences can be problematic on unit-resolution mass spectrometry systems, the ability to collect high-resolution measurements in the field may provide a way to minimize false positive identifications without advanced data analytics.

A complementary area of research focuses on developing algorithms and machine learning (ML) tools to streamline data processing, improve the objectivity of data interpretation, and enable exploratory analyses. Recent advances in uncertainty quantification have produced practical methods for assessing confidence in ML predictions, allowing researchers not only to classify samples but also to evaluate the reliability of those classifications[18]. These approaches will help ensure consistency across laboratories and maximize the information extracted from mass spectrometry data. More broadly, ML-enabled analysis of drug mass spectral signatures could be used to track drug movement across geographic regions or identify emerging opioids before reference spectra become available, enabling public health and law enforcement agencies to respond proactively to changes in the drug supply.

Portable spectroscopy

Alongside efforts to advance portable mass spectrometry, NIST is exploring nascent spectroscopic technologies that enable non-destructive analysis with minimal sample preparation. Within this application domain, multiple spectroscopy-based platforms have been developed for drug screening, including Raman[19–22], infrared[23–25], near-infrared[26], and NMR[27]. Among these techniques, the most widely used are FTIR and Raman spectroscopy, which probe the highly sensitive fundamental vibrational modes of molecules. These modes generate characteristic "molecular fingerprint" spectra, enabling differentiation of structurally similar opioid compounds such as morphine, codeine, oxycodone, and fentanyl. Portable, commercial Raman and FTIR spectrometers are routinely used by customs and law enforcement for rapid screening. Despite their popularity, these generally benchtop devices lack the detection sensitivity and chemical specificity for real street samples where key analytes like fentanyl are present at low concentrations[28], requiring additional validation with mass spectrometry to achieve meaningful accuracy[29]. Finally, FTIR provides limited discrimination of mixture constituents and often require more sophisticated chemometric techniques to detect subtle differences[30].

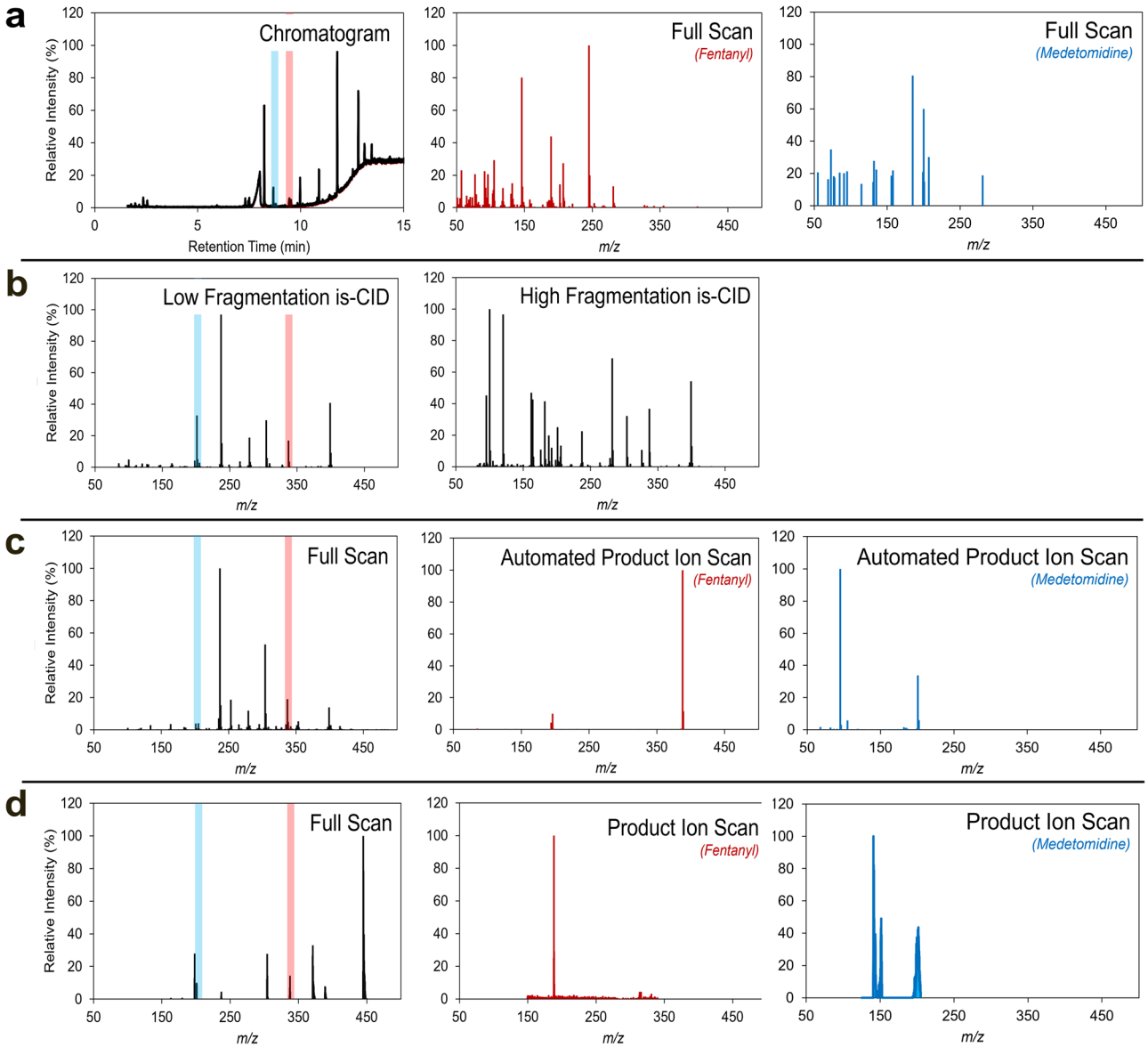

Fig. 1 | Mass spectrometry tools for analyzing drug mixtures. a Traditional gas chromatography-mass spectrometry (GC-MS) of a drug sample containing fentanyl and medetomidine. This analysis requires more than 10 min. **b** Ambient ionization mass spectrometry (AIMS); in this case, direct analysis in real time mass spectrometry (DART-MS). Low/High fragmentation in-source collision-induced dissociation (is-CID) is used to control the level of fragmentation for DART-MS. Next-generation techniques include (**c**) DART coupled with quadrupole time-of-flight mass spectrometry (Q-TOF MS) and **d** portable ion trap mass spectrometry.

Metamaterial-enhanced spectroscopy. Emerging portable technologies capable of near real-time analysis of drug mixtures can transform opioid detection, provided they meet the stringent sensitivity and chemical specificity requirements of real-world samples. For increasing sensitivity, modern advances in signal enhancement, e.g., surface-enhanced Raman spectroscopy (SERS), have achieved a few-percent level detection sensitivity for fentanyl: As an example, electrochemically-driven SERS (EC-SERS) uses roughened metal nanostructures to enhance the Raman signal of drug analytes[22]. Even though synthesis-based (colloidal) nanostructures provide the highest signal enhancement, limitations in sample spatial uniformity and reproducibility are important sources of measurement uncertainties[31,32].

The concept of exploiting signal enhancement from engineered nanostructures has motivated an emerging theme in chemical and biological sensing: metamaterials. Metamaterials represent a powerful and versatile nanophotonic platform for manipulating electromagnetic waves—in amplitude, phase, polarization, direction and spectrum. Flat metamaterials, or metasurfaces, are comprised of structures at the sub-wavelength scale that can confine and amplify electromagnetic fields, enabling dramatic signal enhancements for increasing light-matter interaction. Nanofabrication techniques can now mass produce metamaterial with high uniformity at nanometer resolution, paving a new path towards enhanced detection sensitivity with exceptional reproducibility, not to mention exciting prospects for mass production and device miniaturization. As a new modalities for molecular detection in a small form factor, metasurfaces have seen a growing adoption for surface-enhanced spectroscopy methods: surface-enhanced IR absorption (SEIRA)[33–36] and Raman spectroscopy (SERS)[22,32]. When combined with chip-scale light sources and detectors, the complete infrared integrated photonics system[37] could translate to real-world, field-deployable sensing applications.

Although deployable sensors will ultimately require continued advances in chip-scale infrared light sources and detector readout technologies, the present work focuses on metasurface design—the core element of molecular sensing that largely determines overall sensing performance. Within the field of infrared plasmonics, the generation and control of plasmons provide a versatile platform for surface-enhanced infrared

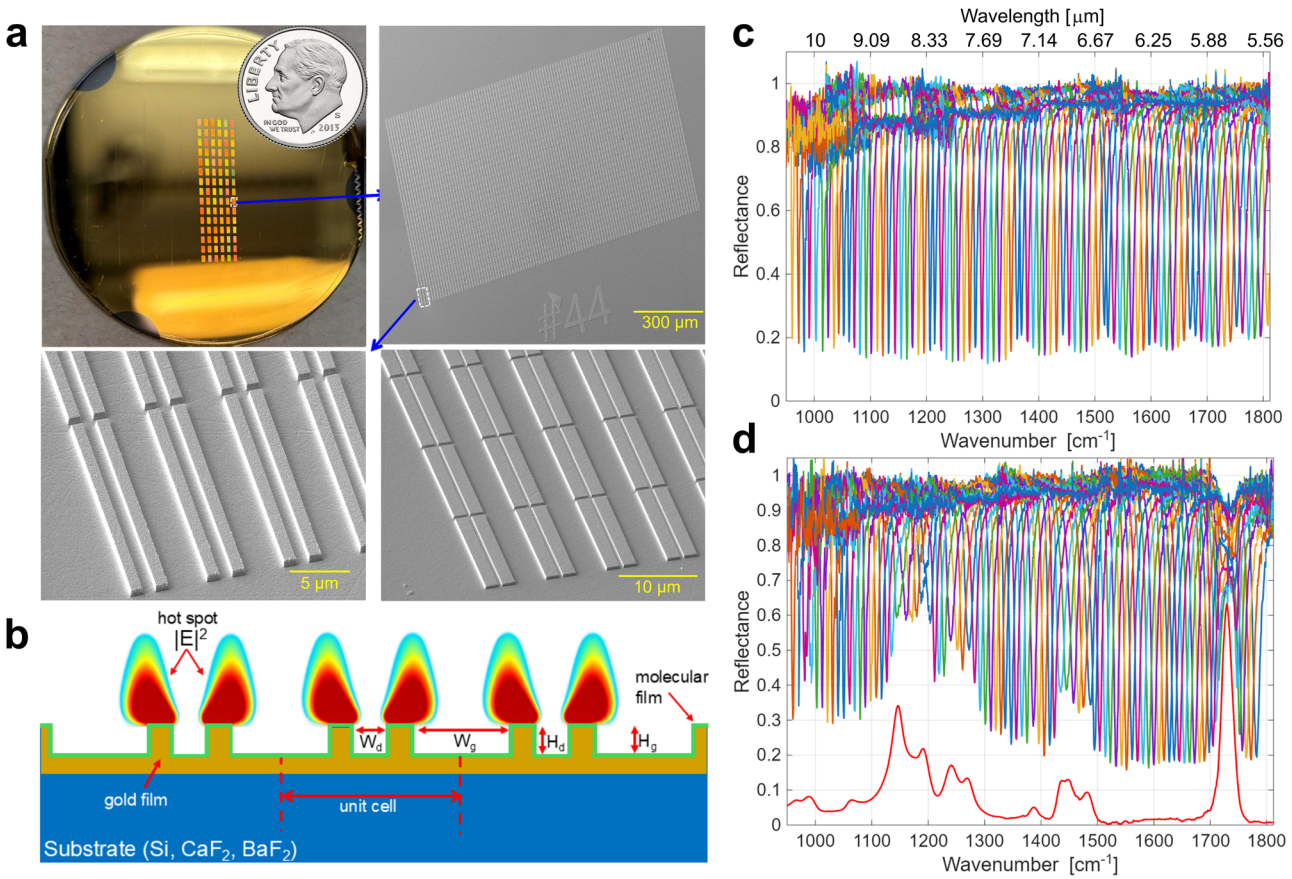

Fig. 2 | Spectroscopy with pixelated metasurfaces. a 90 pixel plasmonic sensor (top left) and scanning electron microscopy (SEM) images at increasing magnification show the periodic nanostructures that form resonant standing waves at IR wavelengths. The highest magnification images (bottom panels) show the nanostructures for two different wavelengths (pixels). **b** Side-view cartoon of the metasurface with labeled design parameters to achieve resonance at target wavelength λ_p. The molecular polymer film for SEIRA spectroscopy is shown in green. The periodic hot spots (COMSOL modeling) are the sites where the electric field is enhanced to increase the light-matter coupling strength and detection sensitivity. **c** 90 pixel spectrum without molecular sample and **d** with 250 nm PMMA polymer. Shown in red is the PMMA FTIR spectrum.

absorption (SEIRA) spectroscopy[38,39]. Here, we adopt gold metasurfaces because of their chemical stability, robustness, and compatibility with the liquid and solid samples commonly encountered in drug sensing. To maximize detection sensitivity across a broad wavelength range, we employ a multi-pixel resonator architecture in which each pixel is designed to achieve maximal electromagnetic field enhancement at a specific wavelength. Our sensor consists of an array of ninety 1 mm × 1.5 mm pixels (Fig. 2a), each engineered to produce a sharp reflection ("resonance") dip at a target wavelength λ_p spanning ≈ 5 to 11 μm. Each pixel is a linear rectangular groove grating patterned by electron beam lithography into an opaque gold film with fixed 500 nm groove depth. Near λ_p, the grating supports a standing plasmonic surface mode, but because a pure Bragg grating (period ≈ $\lambda_p/2$) is dark to free-space excitation, alternating groove widths are slightly perturbed (to W_d and W_g in Fig. 2b) to break symmetry and couple to a quasi-bound-state-in-continuum mode. The structure was optimized using finite-difference time-domain (FDTD) simulations to maximize coupling between normally incident light and a trapped surface plasmon standing wave at target wavelengths. Starting from a non-coupling Bragg reflector geometry with weakly scattering deep-subwavelength grooves, the width of every second groove (W_d) was iteratively reduced to break symmetry, producing near-unity reflection dip and narrow linewidth (Q ≈ 200 to 300) with surface-field enhancement ≈ 50 relative to the incident field. The reproducibility of the sensor fabrication process and molecular responsivity are discussed in Figs. S1–S3 of the Supplementary Information (SI). Additional details of the FDTD simulations used for device design and optimization are presented in Figs. S4–S5 of the SI. By leveraging surface-enhanced infrared spectroscopy using pixelated metasurfaces that span the molecular fingerprint region[40,41], this platform was designed to quantify constituents of complex drug mixtures by their unique spectral signatures.

When coherent light illuminates a pixel, an array of periodic "hot spots" with sub-wavelength scale mode volume is formed as a standing wave, leading to a resonance reflection dip at λ_p. The top panel of Fig. 2c shows the measured reflectance spectrum of the ninety pixel sensor using a pulsed QCL laser (MIRcat, $\lambda \approx 5.5$–10.5 μm) and a MCT detector (VIGO Photonics). To demonstrate molecular detection, spin-coated poly(methyl methacrylate) (PMMA) films were used as a model system. This well-defined polymer system facilitates quantitative analysis by enabling (1) direct determination of the absorption path length from thin-film thickness and (2) development of quantitative models for the analysis of complex mixtures.

When molecules are distributed across the hot spots, their vibrational spectrum is imprinted on the reflectance spectrum of each pixel, as shown in the bottom panel of Fig. 2c. The difference between the reflectance spectra measured with and without molecules is analogous to a conventional FTIR absorption spectrum. In the metasurface structure, however, the periodic array of hot spots drives all molecules in phase, leading to a large number of coupled transitions referred to as a macroscopic collective dipole[42]. When this coherent coupling occurs at the frequency corresponding to the molecular vibrational mode with a strong transition dipole moment, this collective effect manifests as an observed Rabi splitting. This is commonly referred to as the strong-coupling regime. Shown in the bottom panel of Fig. 2c, this splitting is most conspicuous at the C=O stretch molecular transition

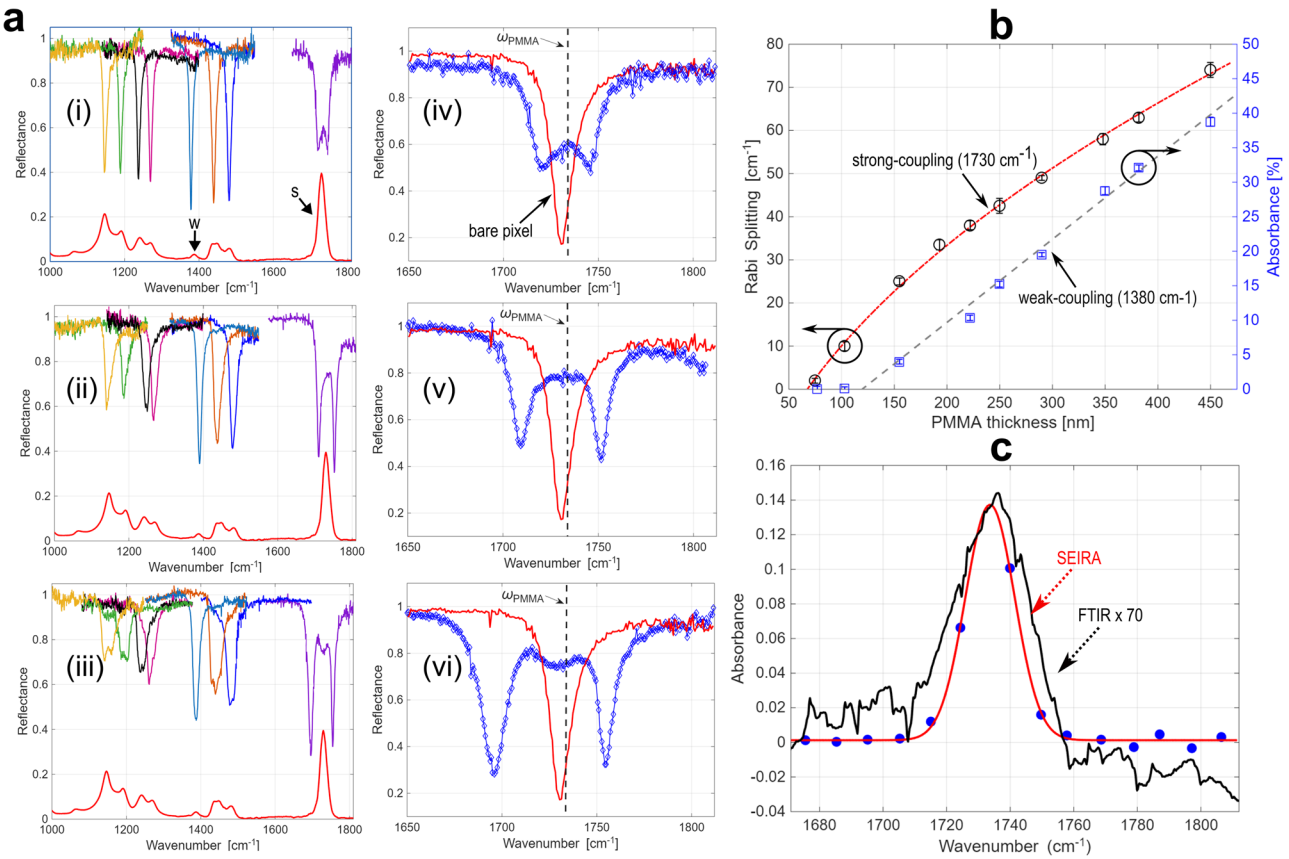

Fig. 3 | Weak- and strong-coupling effects as a function of molecular concentration. a Panels (i–iii) show selected pixels that coincide with molecular absorption features to demonstrate the evolution from weak- to strong-coupling with increasing concentration. Panels (iv–vi) show the zoomed in C=O stretch near 1730 cm^{-1} (vertical dashed line), with the bare pixel overlaid in red to show the Rabi splitting when molecules are introduced. **b** Weak- vs strong-coupling comparison for features indicated by arrows in **a**(i) as a function of increasing PMMA concentration. Rabi splitting of the strongly absorbing feature near 1730 cm^{-1} (`s' in **a**(i)) and fit to $\sqrt{C}$ (red line). Absorbance of the weakly absorbing feature near 1380 $cm^{-1}$ (`w' in **a**(i)) and linear fit (black dashed line). **c** Comparison of the SEIRA absorbance (with metasurface) with reference FTIR absorbance (on gold surface without metasurface) for 78 nm thick PMMA film.

frequency of PMMA near 1730 cm^{-1}. This regime of quantum-based molecular sensing[43,44] occurs when the metasurface resonator and molecules exchange energy faster than dissipative and/or radiative losses, which differs from traditional FTIR and Raman spectroscopy where the probe light only weakly interacts with molecules (perturbative or weak-coupling regime). Strong-coupling has been shown for SEIRA using metasurfaces different from our own: see the following reviews[34,45]. When both the weak-coupling and strong-coupling signatures are simultaneously present, there will be added benefits to detection sensitivity[43], enhanced dynamic range, and molecular specificity for identifying unknown compounds. In the next sections, we discuss the specific advantages in more detail.

(1) Quantitative analysis using traditional absorption spectroscopy relies on the Beer-Lambert law to relate absorbance to molecular concentration. Because absorbance depends linearly on concentration, the usable dynamic range is constrained at high absorbance values—particularly in FTIR measurements within the fingerprint region, where strong transitions are common. Restricting analysis to the linear Beer-Lambert regime (absorbance < 1) and considering a strong vibrational mode such as the C=O stretch, the achievable dynamic range is approximately 10^3-10^4, assuming a typical FTIR absorbance noise floor of 10^{-4}. This limitation can be significant for real-world samples, where potent and potentially toxic adulterants in opioid mixtures may be present at only a few percent concentration.

Measurements over a broad spectral range reveals both weakly- and strongly-coupled features in the PMMA absorption spectrum. Figure 3a shows some selected pixels that highlight the weak- and strong-coupling features at three different PMMA polymer thickness: 155 nm (i and iv), 250 nm (ii and v), and 350 nm (iii and vi). The strong-coupling splitting as a function of increasing concentration is most apparent in panels iv to vi. By observing signals from weak-coupling (linear absorption) and strong-coupling (Rabi splitting), we can extend the detection dynamic range to $>10^4$ by achieving low noise ($\approx 1 \times 10^{-4}$) on the low absorbance end while extending the dynamic range on the high absorbance from strong-coupling. Figure 3b shows the linear absorption (weak-coupling feature) and the square-root dependence of the Rabi splitting (strong-coupling feature) as a function of PMMA concentration (thickness). Whereas the linear absorption feature near 1380 cm^{-1} is approaching the saturation limit of Beer-Lambert ($\approx$ 50% absorbance), the Rabi splitting continues to increase $\approx \sqrt{C}$ and is only limited by the wavelength coverage of our laser to measure both the upper and lower branches of the Rabi splitting. The detection limit for the PMMA polymer film is approximately 50 nm in thickness, defined as the point at which a change can be observed in the strong C=O stretching band near 1730 cm^{-1}. The limit of quantification is approximately 78 nm, at which both weakly and strongly absorbing spectral features can be observed across the entire measured spectral range (5.5–10.5 μm). Finally, it is instructive to compare the increased molecular detection sensitivity based on SEIRA compared to traditional absorption spectroscopy (e.g., FTIR). This SEIRA enhancement factor, defined as a ratio of the absorbance with a metasurface to a reference absorbance without a metasurface, is $\approx$ 70 by using the C=O stretch mode of 78 nm thick PMMA film (Fig. 3c). Note that this comparison is only valid in the weak-coupling regime where the resonator and molecule retain their individual characteristics (coupling between molecules and resonator mode is a weak perturbation). Rabi splitting in the strong-coupling regime has no direct analogue to traditional linear absorption spectroscopy.

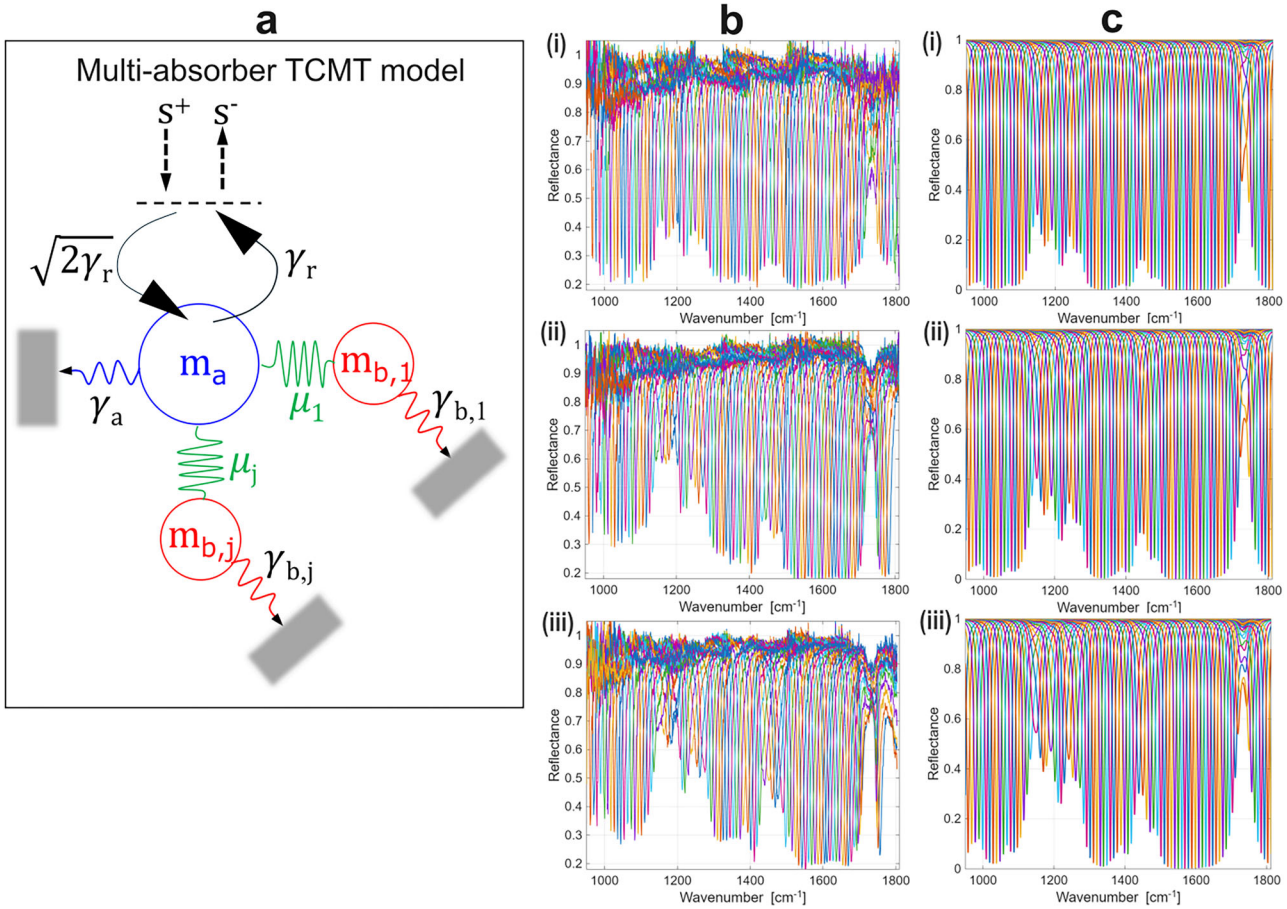

Fig. 4 | Multi-absorber temporal coupled-mode theory for quantitative analysis. **a** Schematic for the multi-absorber TCMT model. A resonator with mass m_a couples to different absorbers with mass $m_{b,1}$ to $m_{b,j}$ where $j = 1$: M by the coupling constant μ_j. **b** Experimental spectrum for (i) 155 nm, (ii) 250 nm, and (iii) 350 nm thick PMMA (top to bottom). **c** Calculated spectrum for data in (**b**) using the reflectance function from Eq. (2) with molecular concentration as the only adjustable parameter. The concentration ratios correspond to the PMMA thickness ratios in (**b**).

To obtain quantitative information for the analysis of complex mixtures, we developed a theoretical model for interpreting SEIRA spectra. When molecules are located within the resonator's mode volume, they modify the resonance response through their contribution to the effective permittivity and absorption losses of the resonator. To model this behavior, we begin with the base temporal coupled-mode theory model[35,36] (TCMT, Fig. 4a) that describes a single resonator mode a (with angular frequency ω_r and losses γ_r and γ_a) coupled to a single molecular mode b (with angular frequency ω_b and loss γ_b) via the coupling term μ. s^+ and s^- are the incident and reflected fields, respectively. The presence of multiple molecular species, each possessing distinct vibrational modes, further perturbs the resonator response. In the multi-absorber TCMT framework, this effect is incorporated by (1) introducing additional absorber modes and (2) explicitly including a molecular concentration (C) dependence in both the sample's effective bulk refractive index and the coupling parameter, μ. The former produces a trivial frequency shift arising from mass-loading-induced changes in the bulk refractive index, whereas the latter effect dominates when $\omega_r \approx \omega_b$. Assuming there are M independent molecular absorbers with concentration C_j (j = 1, …, M) coupling to a single resonator mode a, the resulting multi-absorber TCMT model is given by:

$$\begin{cases} \frac{da}{dt} = -i[\omega_r + \alpha C_{tot}]a - (\gamma_r + \gamma_a)a + i\sum_{j=1}^{M}\mu_j b_j + \sqrt{2\gamma_r}\, s^+, \\ \frac{db_j}{dt} = -i\omega_{b,j} b_j - \gamma_{b,j} b_j + i\mu_j a, \\ s^- = -s^+ + \sqrt{2\gamma_r}\, a. \end{cases} \quad (1)$$

Here $\Delta\omega_r(C) = \alpha C_{tot}$ describes the resonator frequency shift as a function of total molecular concentration, expressed through the effective refractive index (n_{eff}). The magnitude of the shift depends on the proportionality constant $\alpha = dn_{\text{eff}}/dC_{\text{tot}}$. The concentration-dependence of strong-coupling is introduced via the resonator-molecule coupling term $\mu_j = \sqrt{C_j}$, since intrinsic resonator losses (γ_a and γ_r) are unaffected by the introduction of molecules. Finally, an analytical expression for the reflectance function ($r = s^-/s^+$) is derived for direct comparison with experimental reflectance data:

$$r(\omega) = -1 + \frac{2\gamma_r}{i(\omega - [\omega_r + \alpha C_{tot}] - \Omega_\mu) + (\gamma_r + \gamma_a + \Gamma_\mu)} \quad (2)$$

where

$$\Omega_\mu(\omega) = \sum_{j=1}^{M} \frac{\mu_j(\omega - \omega_{b,j})}{(\omega - \omega_{b,j})^2 + \gamma_{b,j}^2}, \quad (3)$$

$$\Gamma_\mu(\omega) = \sum_{j=1}^{M} \frac{\mu_j \gamma_{b,j}}{(\omega - \omega_{b,j})^2 + \gamma_{b,j}^2}. \quad (4)$$

Figure 4b, c compare the experimental and simulated spectra (computed using Eqs. (2)–(4)), respectively, assuming a linear scaling of concentration with PMMA film thickness.

(2) Achieving molecular specificity to identify unknown, and potentially emergent substances is a longstanding goal in drug forensics. As drug trafficking naturally evolves to reflect the changing supply/

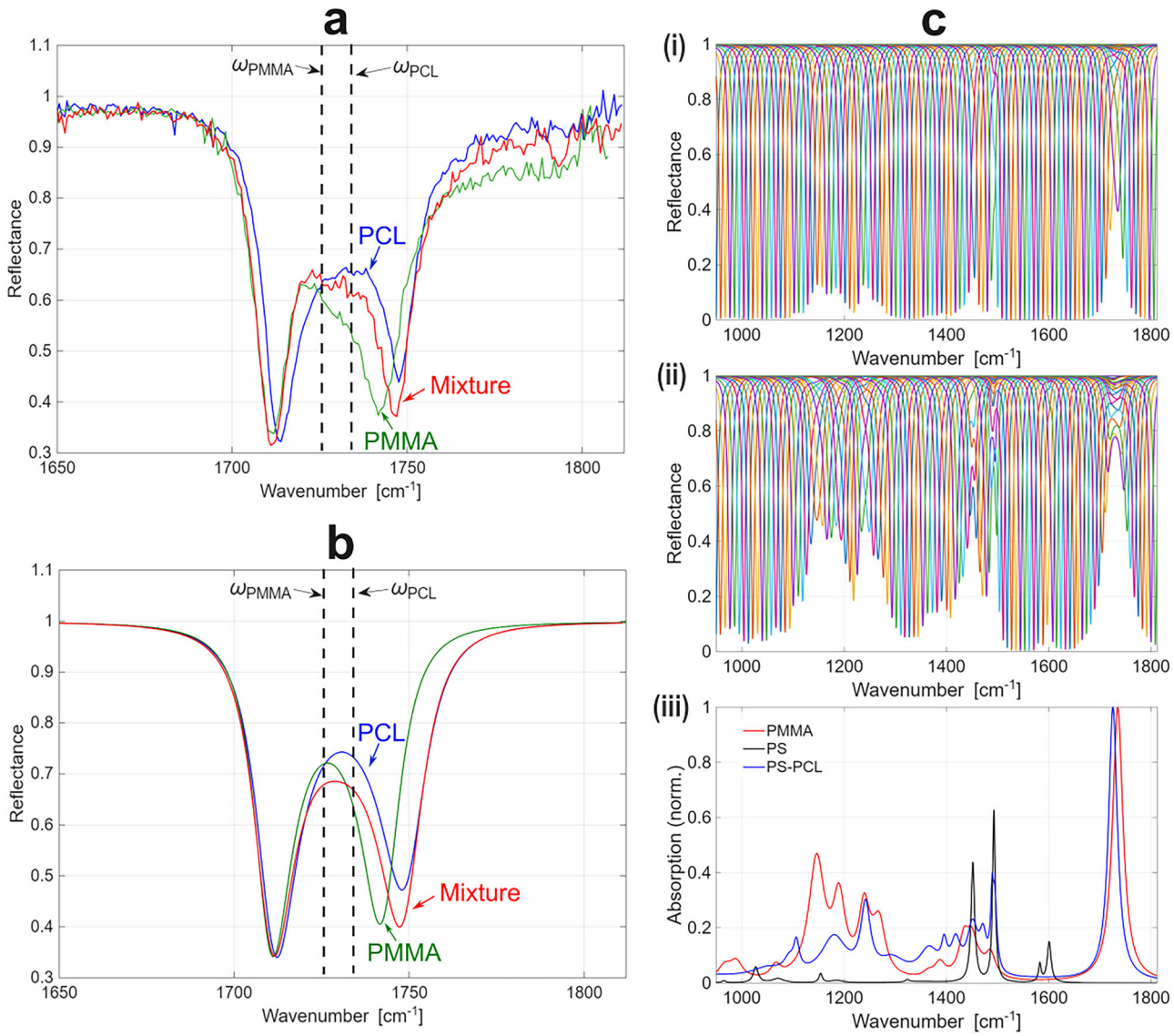

Fig. 5 | Resolving molecular mixtures from strong-coupling signatures. **a** Experimental spectra of the pixel in the C=O stretch region for a mixture of polystyrene: polycaprolactone:poly(methyl methacrylate) or PS:PCL:PMMA. **b** Simulations of PS:PCL:PMMA mixture in (**a**). **c**(iii) shows the absorption spectrum for the three polymers used to calculate the reflectance in (i) and (ii) for a 1:1:1 concentration ratio. The concentration for data in (ii) is double of that in (i).

demand dynamics and regulatory landscape, new compounds are rapidly introduced into circulation that compel immediate action[46]. Rapidly evolving drug supplies across large geographic regions pose significant challenges for analytical instruments requiring high sensitivity, wide dynamic range, and rapid measurement of complex mixtures. Modern metamaterial-based sensing platforms, such as our pixelated plasmonic metasurfaces, are fully configurable and offer a promising pathway to meet these demands. As an example, we have introduced a mixture of PMMA, polystyrene (PS), and polycaprolactone (PCL) polymer. PMMA and PCL polymers have strong C=O vibrational transitions near 1730 cm^{-1}, but are slightly shifted from one another by about 5 cm^{-1}. Figure 5a shows a clear distinctive shift in the strong-coupling splittings for PCL and PMMA polymers, indicating that the Rabi splitting can differentiate the two despite the close proximity of their transition frequencies. TCMT simulations in Fig. 5b reproduces this shift. Figure 5c is a simulated concentration dependence of the three polymer mixture based on the TCMT model that again reveals the richness of both weak- and strong-coupling signatures across the whole molecular fingerprint region. We note that, although the TCMT framework has thus far seen limited validation using real drug samples, our refinement of the model for molecular analysis demonstrates its potential utility for quantitative SEIRA spectroscopy.

Despite their utility for benchmarking sensor performance, spin-coated polymers do not accurately capture the complexity of real drug samples or the ways in which such samples are collected and analyzed in the field. We present initial results showing that our drug-sensing approach remains effective under a more realistic sampling scheme using drop-cast ibuprofen. Because ibuprofen exhibits a strong C=O stretching mode similar to those of PMMA and PCL, it serves as an ideal test case for demonstrating strong coupling with drop-cast sample preparation. Figure 6a shows the bare sensor and the sensor after deposition of 20 µl of ibuprofen dissolved in acetonitrile. After the solvent evaporates, a solid ibuprofen film remains, covering the entire sensor area. Figure 6b presents the reflectance spectra for three different ibuprofen concentrations, expressed as mass normalized to a 1 mm^2 pixel area. Despite the less controlled sampling methodology compared to spin-coated polymer films, we successfully achieved chemical sensing in the strong-coupling regime. The inset demonstrates a similar square-root dependence on concentration. However, because the drop-cast method is susceptible to sampling-induced systematic uncertainties, we defer reporting detection

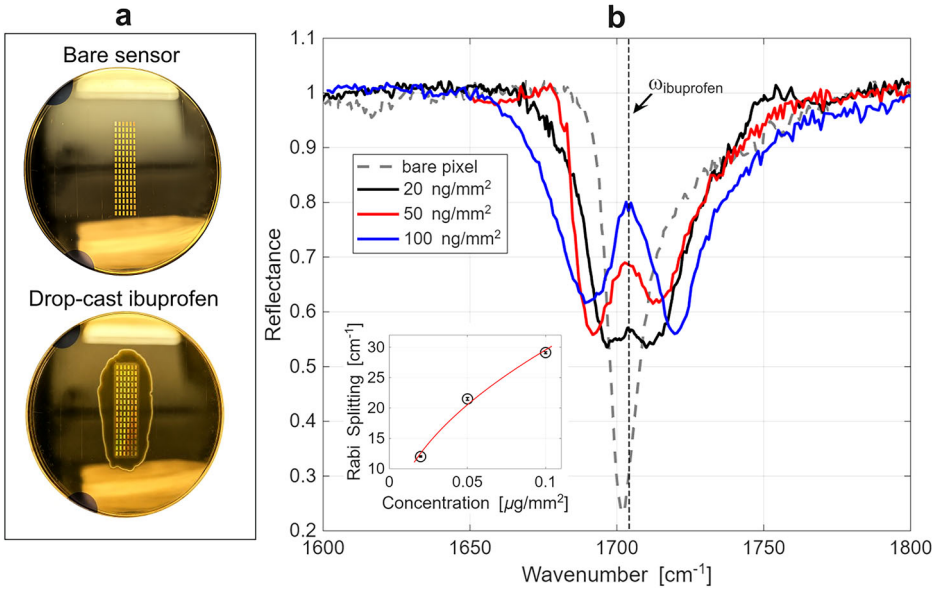

Fig. 6 | Strong-coupling effects in drop-cast ibuprofen. a Twenty microliters of ibuprofen dissolved in acetonitrile were drop-cast onto the metasurface sensor, leaving behind a dry film covering all 90 pixels. **b** Reflectance spectra of a pixel near the C=O stretch transition ($\omega_{ibuprofen}$) as a function of molecular concentration (black = 20 ng/mm^2, red = 50 ng/mm^2, and blue = 100 ng/mm^2). The gray dashed line shows the spectrum of a bare pixel without molecules. The inset shows the Rabi splitting as a function of concentration; the red line is a square-root fit.

metrics until a comprehensive quantitative analysis is conducted in follow-up work.

As strong-coupling depends on molecular concentration, increasing the amount of deposited material from real samples is straightforward and can be accomplished by applying additional aliquots of a dissolved sample to the metasurface sensor. For street-level drug samples, however, the primary challenge is not necessarily extremely low analyte concentrations, but rather the substantial variability in both the concentrations of individual components and the number of different components present in a mixture. According to NIST's RaDAR database (https://content.govdelivery.com/accounts/USNIST/bulletins/416d5ef.), drug samples collected in 2026 had a median fentanyl concentration of 7% by weight, with concentrations reaching nearly 30% in some samples. In most cases, these drug mixtures contained more than ten components. Nevertheless, this initial demonstration suggests that a practical drop-casting-based drug sampling method can benefit from enhanced sensing performance, particularly when weak- and strong-coupling effects are observed within the same detection platform.

Mobile testing platform

Implementation of new technology for drug detection and identification can be a difficult task. Even if cost, training, and spectral library barriers are overcome, new technology has to be demonstrated as fit-for-purpose using real-world samples in operationally relevant scenarios. This can be difficult for industry to access and navigate. To address this need, NIST is currently developing a deployable mobile testing laboratory equipped with portable mass spectrometry and spectroscopy tools. In addition to the instrumentation housed within the mobile laboratory, larger vehicle-mounted mass spectrometry systems with full laboratory-grade capabilities will be used to better understand the limitations of portable devices through the simultaneous analysis of samples on both portable and laboratory-grade platforms.

Once completed, the mobile laboratory will provide the necessary controls and safety features to enable in-field analysis of drug samples. The laboratory is designed to allow rapid interchange of instrumentation, enabling researchers and industry partners to evaluate how analytical equipment performs under real-world field conditions. By collaborating with stakeholder communities (i.e., law enforcement agencies and harm reduction organizations), analysis of real-world samples using a variety of validated and next-generation technologies can occur in real-time, closing a critical loophole in the research and development and ensuring technology being developed can adequately meet the needs of the community.

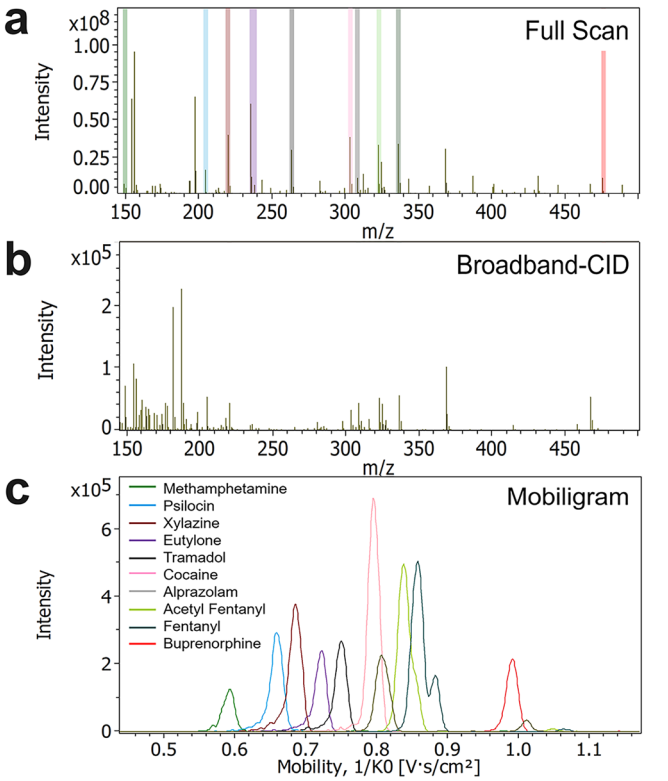

Fig. 7 | Ion mobility mass spectrometry. Implementing ion mobility tools provides an additional dimension of data without increasing analysis time. In this example, a ten compound mixture is analyzed by DART trapped ion mobility quadrupole time-of-flight mass spectrometry (DART-timsTOF). **a** Full scan mass spectrum. **b** Broadband collision induced dissociation (CID) spectrum. **c** Extracted ion mobiligram for the protonated molecules for each of the ten listed compounds. Data for the sample was collected in under ten seconds.

Future directions

While developing tools to lower implementation barriers of new mass spectrometry and spectroscopy tools remains a priority, ongoing and future research efforts in this space are more focused on increasing speed, enhancing specificity, and extracting maximum data from a single measurement. To accelerate the adoption of mature mass spectrometry, we are

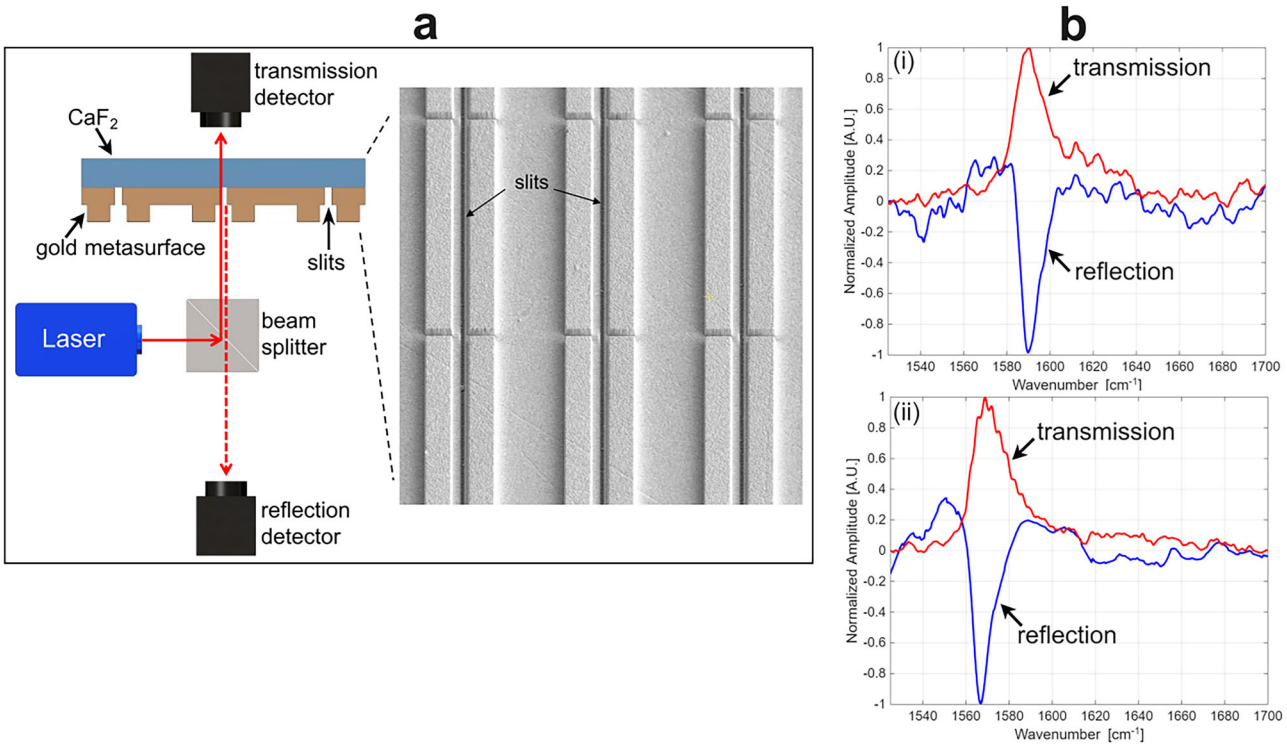

Fig. 8 | Transmission-based metasurface sensor. a Measurement of reflection/transmission mode sensor with gold metasurface on calcium fluoride (CaF_2) substrate. SEM image shows the slits introduced by focused ion beam (FIB) milling in between the grooves of the plasmonic nanostructures for transmission measurements. **b** Transmission and reflection spectra of two pixels with different λ_p, as shown in (i) and (ii).

actively investigating the use of AI-MS for simultaneous qualitative and quantitative analysis of sample-providing information to end-users on how much opioid is present in a sample, not just which opioid. One ongoing strategy is to increase the data rate for gas chromatography (GC) and liquid chromatography (LC) with mass spectrometry. Recently, rapid gas chromatography-mass spectrometry (GC-MS) methods were validated and implemented using rapid-heating ovens, reducing the chromatographic run time to under two minutes[47]. In addition, the use of separation or pseudo-separation techniques such as ion mobility or ramped thermal desorption could provide further dimensionality to the data-increasing specificity without significantly increasing analysis time (see Fig. 7).

To potentially reduce cost, size, and measurement time, our spectroscopy-based efforts are focused on exploring an imaging-based metasurface sensor platform where all pixels are viewed by a cost-effective microbolometer camera, enabling single shot measurement of the broadband spectrum in under 1 s. A current limitation of reflection-mode detection is the high background brightness from the IR source, which can overwhelm the reflection contrast of each pixel when imaged on a camera (bright-field mode). As shown in Fig. 8, incorporating transmission slits into the grooves of the plasmonic pixels converts the device to transmission mode, enabling dark-field spectroscopy and enhancing the spectral contrast of the resonator relative to the background.

Finally, the area for greatest advancement, however, is in improving data analytics. Using novel algorithms[48–51], machine learning models, and uncertainty quantification to drive novel opioid discovery could enable the community to be alerted to new drugs in the supply more quickly. Moreover, such techniques can provide actionable information about when additional scrutiny or measurement of a sample is required, e.g., when its status as an opioid is uncertain. Merging spectral data with metadata (geographic location, sample type, sample markings, etc.) could increase our knowledge of how samples move - enabling predictive analytics that could allow public health entities to proactive position resources that minimize the negative impacts of this epidemic.

Data availability

All data generated or analyzed during this study are included in this published article and its Supplementary Information files and can be made available from the corresponding author on reasonable request.

Received: 27 February 2026; Accepted: 17 July 2026;
Published online: 29 July 2026

References

1. Robert, M., Jouanjus, E., Khouri, C., Fouilhé Sam-Laï, N. & Revol, B. The opioid epidemic: a worldwide exploratory study using the who pharmacovigilance database. *Addiction* **118**, 771–775 (2023).
2. Garnett, M. & Minino, A. Drug overdose deaths in the united states, 2023–2024. NCHS Data Brief, no 549 https://www.cdc.gov/nchs/data/databriefs/db549.pdf (2024).
3. U.S. Joint Economic Committee. The economic toll of the opioid crisis reached nearly $1.5 trillion in 2020. Issue Brief https://www.jec.senate.gov/public/_cache/files/67bced7f-4232-40ea-9263-f033d280c567/jec-cost-of-opioids-issue-brief.pdf (2022).
4. Joshi, M. & Sisco, E. Forensic seized drug analysis: current challenges and emerging analytical solutions. *WIREs Forensic Sci.* **5**, e1486 (2023).
5. Stangeland, M., Dale, O. & Skulberg, A. K. Nitazenes: review of comparative pharmacology and antagonist action. *Clin. Toxicol.* **63**, 393–406 (2025).
6. Lenzi, M. et al. New synthetic opioids: What do we know about the mutagenicity of brorphine and its analogues? *Int. J. Mol. Sci*. **26**, 5084, https://www.mdpi.com/1422-0067/26/11/5084 (2025).
7. Ahmed, R., Altamimi, M. J. & Hachem, M. State-of-the-art analytical approaches for illicit drug profiling in forensic investigations. *Molecules* **27**, 6602, https://www.mdpi.com/1420-3049/27/19/6602 (2022).
8. Philp, M. & Fu, S. A review of chemical 'spot' tests: A presumptive illicit drug identification technique. *Drug Test. Anal.* **10**, 95–108 (2018).

9. Halifax, J. C., Lim, L., Ciccarone, D. & Lynch, K. L. Testing the test strips: laboratory performance of fentanyl test strips. *Harm Reduct. J.* **21**, 14 (2024).
10. Henderson, A., Heaney, L. M. & Rankin-Turner, S. Ambient ionisation mass spectrometry for drug and toxin analysis: a review of the recent literature. *Drug Test. Anal.* **16**, 1323–1344 (2024).
11. Cody, R. B., Laramée, J. A. & Durst, H. D. Versatile new ion source for the analysis of materials in open air under ambient conditions. *Anal. Chem.* **77**, 2297–2302 (2005).
12. Sisco, E. & Forbes, T. P. Forensic applications of Dart-MS: a review of recent literature. *Forensic Chem.* **22**, 100294 (2021).
13. Sisco, E., Burns, A., Schneider, E., Bobka, L. & Ikpeama, I. A template for the validation of Dart-MS for qualitative seized drugs analysis. *Forensic Chem.* **29**, 100415 (2022).
14. Sisco, E., Moorthy, A. S. & Watt, L. M. Creation and release of an updated NIST Dart-MS forensics database. *J. Am. Soc. Mass Spectrom.* **32**, 685–689 (2021).
15. Moorthy, A. S. & Sisco, E. A new library-search algorithm for mixture analysis using Dart-MS. *J. Am. Soc. Mass Spectrom.* **32**, 1725–1734 (2021).
16. Sisco, E., Appley, M. G., Tennyson, S. S. & Moorthy, A. S. Qualitative analysis of real drug evidence using Dart-MS and the inverted library search algorithm. *J. Am. Soc. Mass Spectrom.* **33**, 1784–1793 (2022).
17. Forbes, T. P., Robinson, E. L., Sisco, E. & Koss, A. A point-of-need framework for illicit drug identification with high-resolution mass spectrometry. *Analyst* **150**, 1578–1589 (2025).
18. Patrone, P. & Kearsley, A. Probabilistic consistency in machine learning and its connection to uncertainty quantification. Preprint at https://arxiv.org/abs/2507.21670 (2025).
19. Turzhitsky, V. et al. Picoanalysis of drugs in biofluids with quantitative label-free surface-enhanced raman spectroscopy. *Small* **14**, 1802392 (2018).
20. Azimi, S. & Docoslis, A. Recent advances in the use of surface-enhanced raman scattering for illicit drug detection. *Sensors* **22**, 3877, https://www.mdpi.com/1424-8220/22/10/3877 (2022).
21. Ott, C. E., Burns, A., Sisco, E. & Arroyo, L. E. Targeted fentanyl screening utilizing electrochemical surface-enhanced raman spectroscopy (ec-sers) applied to authentic seized drug casework samples. *Forensic Chem.* **34**, 100492 (2023).
22. Ott, C. E. et al. Development and evaluation of a nontargeted electrochemical surface-enhanced Raman spectroscopy (ec-sers) screening method applied to forensic seized drug casework samples. *Forensic Chem.* **41**, 100621 (2024).
23. Green, T. C. et al. An assessment of the limits of detection, sensitivity and specificity of three devices for public health-based drug checking of fentanyl in street-acquired samples. *Int. J. Drug Policy* **77**, 102661 (2020).
24. McCrae, K. et al. Assessing the limit of detection of Fourier-transform infrared spectroscopy and immunoassay strips for fentanyl in a real-world setting. *Drug Alcohol Rev.* **39**, 98–102 (2020).
25. Goncalves, R. et al. Suitability of infrared spectroscopy for drug checking in harm reduction centres. *Int. J. Drug Policy* **88**, 103037 (2021).
26. Kranenburg, R. F. et al. On-site illicit-drug detection with an integrated near-infrared spectral sensor: a proof of concept. *Talanta* **245**, 123441 (2022).
27. Draper, S. L. & McCarney, E. R. Benchtop nuclear magnetic resonance spectroscopy in forensic chemistry. *Magn. Reson. Chem.* **61**, 106–129 (2023).
28. Alonzo, M., Alder, R., Clancy, L. & Fu, S. Portable testing techniques for the analysis of drug materials. *WIREs Forensic Sci.* **4**, e1461 (2022).
29. Cooman, T. et al. Screening of seized drugs utilizing portable Raman spectroscopy and direct analysis in real time-mass spectrometry (Dart-MS). *Forensic Chem.* **25**, 100352 (2021).
30. Zarnowiec, P., Lechowicz, L., Czerwonka, G. & Kaca, W. Fourier transform infrared spectroscopy (FTIR) as a tool for the identification and differentiation of pathogenic bacteria. *Curr. Med. Chem.* **22**, 1710–1718 (2015).
31. Smith, M. et al. A semi-quantitative method for the detection of fentanyl using surface-enhanced Raman scattering (SERS) with a handheld Raman instrument. *J. Forensic Sci.* **66**, 505–519 (2021).
32. Zhu, Y. et al. On-site quantitative detection of fentanyl in heroin by machine learning-enabled SERS on super absorbing metasurfaces. *npj Nanophotonics* **2**, 7 (2025).
33. Wang, H.-L., You, E.-M., Panneerselvam, R., Ding, S.-Y. & Tian, Z.-Q. Advances of surface-enhanced Raman and ir spectroscopies: from nano/microstructures to macro-optical design. *Light Sci. Appl.* **10**, 161 (2021).
34. John-Herpin, A. et al. Metasurface-enhanced infrared spectroscopy: an abundance of materials and functionalities. *Adv. Mater.* **35**, 2110163 (2023).
35. Adato, R., Artar, A., Erramilli, S. & Altug, H. Engineered absorption enhancement and induced transparency in coupled molecular and plasmonic resonator systems. *Nano Lett.* **13**, 2584–2591 (2013).
36. Paggi, L. et al. Over-coupled resonator for broadband surface enhanced infrared absorption (SEIRA). *Nat. Commun.* **14**, 4814 (2023).
37. Mitchell, C. J. et al. Mid-infrared silicon photonics: from benchtop to real-world applications. *APL Photonics* **9**, 080901 (2024).
38. Stanley, R. Plasmonics in the mid-infrared. *Nat. Photonics* **6**, 409–411 (2012).
39. Liang, Y., Tsai, D. P. & Kivshar, Y. From local to nonlocal high-*q* plasmonic metasurfaces. *Phys. Rev. Lett.* **133**, 053801 (2024).
40. Tittl, A. et al. Imaging-based molecular barcoding with pixelated dielectric metasurfaces. *Science* **360**, 1105–1109 (2018).
41. Richter, F. U. et al. Gradient high-q dielectric metasurfaces for broadband sensing and control of vibrational light-matter coupling. *Adv. Mater.* **36**, 2314279 (2024).
42. Shalabney, A. et al. Coherent coupling of molecular resonators with a microcavity mode. *Nat. Commun.* **6**, 5981 (2015).
43. Zheng, P., Semancik, S. & Barman, I. Quantum plexcitonic sensing. *Nano Lett.* **23**, 9529–9537 (2023).
44. Zheng, P., Semancik, S. & Barman, I. Quantum vibropolaritonic sensing. *Sci. Adv.* **11**, eady7670 (2025).
45. Kozuch, J., Ataka, K. & Heberle, J. Surface-enhanced infrared absorption spectroscopy. *Nat. Rev. Methods Prim.* **3**, 70 (2023).
46. Hochstatter, K. et al. Characterizing rapid changes in the prevalence and concentration of key compounds in Philadelphia's street opioid retail supply, march 2024-march 2025. *Drug Alcohol Depend.* **274**, 112763 (2025).
47. Capistran, B. A. & Sisco, E. Validation of a rapid gc–ms method for forensic seized drug screening applications. *Forensic Chem.* **41**, 100609 (2024).
48. Tittl, A., John-Herpin, A., Leitis, A., Arvelo, E. R. & Altug, H. Metasurface-based molecular biosensing aided by artificial intelligence. *Angew. Chem. Int. Ed.* **58**, 14810–14822 (2019).
49. Ayres, L. B., Gomez, F. J., Linton, J. R., Silva, M. F. & Garcia, C. D. Taking the leap between analytical chemistry and artificial intelligence: a tutorial review. *Anal. Chim. Acta* **1161**, 338403 (2021).
50. Roberts, M. J., Moorthy, A. S., Sisco, E. & Kearsley, A. J. Incorporating measurement variability when comparing sets of high-resolution mass spectra. *Anal. Chim. Acta* **1230**, 340247 (2022).
51. Krishnaswamy-Usha, A., Capistran, B. A. & Kearsley, A. J. Novel probabilistic similarity scores for sets of replicate ei mass spectra. *Anal. Chim. Acta* **1351**, 343858 (2025).

Acknowledgements

We acknowledge funding support from the NIST SERI program. We thank Eric Norrgard and Kevin Cossel for reading the manuscript and providing helpful suggestions. Reference is made to commercial products to adequately specify the experimental procedures involved. Such identification does not imply recommendation or endorsement by the

National Institute of Standards and Technology, nor does it imply that these products are the best for the purpose specified.

Author contributions

T.B. and H.L. conceptualized the original idea and method. H.L. designed the metasurface sensor. T.B. and K.D. conducted the spectroscopy measurements. W.Z., J.S., and D.F. fabricated the metasurface sensor devices. E.S. performed mass spectrometry measurements of opioids. A.K. conducted statistical modeling and uncertainty quantification. All authors reviewed the manuscript.

Competing interests

The authors declare no competing interests.

Additional information

Supplementary information The online version contains supplementary material available at https://doi.org/10.1038/s44328-026-00112-y.

Correspondence and requests for materials should be addressed to Thinh Q. Bui.